

PuzzleAvatar: Assembling 3D Avatars from Personal Albums

YULIANG XIU, Max Planck Institute for Intelligent Systems, Germany

YUFEI YE, Max Planck Institute for Intelligent Systems, Germany and Carnegie Mellon University, USA

ZHEN LIU, Max Planck Institute for Intelligent Systems, Germany and Mila, Université de Montréal, Canada

DIMITRIOS TZIONAS, University of Amsterdam, Netherlands

MICHAEL J. BLACK, Max Planck Institute for Intelligent Systems, Germany

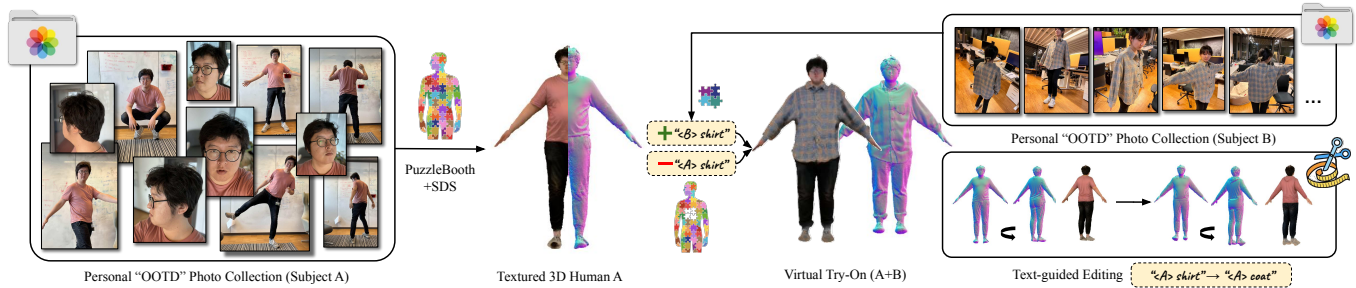


Fig. 1. PuzzleAvatar reconstructs a faithful, personalized, textured 3D human avatar from a personal photo collection. That is, it takes as input a set of “OOTD” (Outfit Of The Day) personal photos with unconstrained body poses, camera poses, framing, lighting and backgrounds, albeit with a consistent outfit and hairstyle. All these consistent factors are learned as separate unique tokens $\langle \text{asset } X \rangle$ in a compositional manner, like pieces of a puzzle. PuzzleAvatar allows us easily inter-change tokens for downstream tasks, such as for customizing avatars and performing virtual try-on while preserving identity, see [video](#).

Generating **personalized** 3D avatars is crucial for AR/VR. However, recent text-to-3D methods that generate avatars for celebrities or fictional characters, struggle with everyday people. Methods for faithful reconstruction typically require full-body images in controlled settings. What if users could just upload their personal “OOTD” (Outfit Of The Day) photo collection and get a faithful avatar in return? The challenge is that such casual photo collections contain diverse poses, challenging viewpoints, cropped views, and occlusion (albeit with a consistent outfit, accessories and hairstyle). We address this novel “**Album2Human**” task by developing **PuzzleAvatar**, a novel model that generates a faithful 3D avatar (in a canonical pose) from a personal OOTD album, bypassing the challenging estimation of body and camera pose. To this end, we fine-tune a foundational vision-language model (VLM) on such photos, encoding the appearance, identity, garments, hairstyles, and accessories of a person into separate learned tokens, instilling these cues into the VLM. In effect, we exploit the learned tokens as “puzzle pieces” from which we assemble a faithful, personalized 3D avatar. Importantly, we can customize avatars by simply inter-changing tokens. As a benchmark for this new task, we create a new dataset, called **PuzzleIOI**, with 41 subjects in a total of nearly 1k OOTD configurations, in challenging partial photos with paired ground-truth 3D bodies. Evaluation shows that PuzzleAvatar not only has high reconstruction accuracy, outperforming TeCH and MVDreamBooth, but also a unique scalability to album photos, and has demonstrating strong robustness. Our model and data will be public.

CCS Concepts: • **Computing methodologies** → *Appearance and texture representations*; **Reconstruction**; *Shape inference*.

Additional Key Words and Phrases: Text-to-Image Diffusion Model, Image-based Modeling, Text-guided 3D Generation, Digital Human

Authors’ addresses: Yuliang Xiu, yuliang.xiu@tuebingen.mpg.de, Max Planck Institute for Intelligent Systems, Germany; Yufei Ye, yeyf13.judy@gmail.com, Max Planck Institute for Intelligent Systems, Germany and Carnegie Mellon University, USA; Zhen Liu, zhen.liu@tuebingen.mpg.de, Max Planck Institute for Intelligent Systems, Germany and Mila, Université de Montréal, Canada; Dimitrios Tzionas, d.tzionas@uva.nl, University of Amsterdam, Netherlands; Michael J. Black, black@tuebingen.mpg.de, Max Planck Institute for Intelligent Systems, Germany.

1 INTRODUCTION

In all chaos there is a cosmos, in all disorder a secret order.

CARL JUNG

Advances in text-guided digital human synthesis open the door to 3D avatar creation with arbitrary skin tones, clothing styles, hairstyles and accessories. While these advances have demonstrated great potential by generating iconic figures (such as Superman or Bruce Lee) and editing specific human features (such as wavy hair or full beards), the problem of crafting one’s *personalized* full-body avatar is relatively unexplored. Imagine that you are given a personal “outfit of the day” (OOTD) photo album in casual snapshots: strolling through a park, crouching to tie a shoelace, seated at a cafe, etc. These snapshots, capturing full-body actions, upper-body poses and close-up selfies with diverse backgrounds, lighting and camera settings, form a rich photo collection. Notably, this collection is relatively “unconstrained”, that is, its only constraint is having a consistent identity, outfit, hairstyle and accessories, while every other factor can vary arbitrarily; see Fig. 1. Can we effectively construct from this album a personalized 3D avatar that vividly characterizes the user’s clothes, physique, and facial details? In this work, we investigate this novel task, which we call “**Album2Human**”, that transforms everyday album collections into textured 3D humans.

Compared to work that reconstructs general 3D scenes from photos with varying lighting conditions, cropping ratio, background and camera settings [Martin-Brualla et al. 2021; Sun et al. 2022], **Album2Human** is more challenging due to the additional factor of varying body articulation. On the other hand, **Album2Human** drastically differs from prior work [Alldieck et al. 2018b; Peng et al. 2023; Vlasic et al. 2009] that creates personalized avatars from images captured in laboratory settings [Cheng et al. 2023; Işık et al.

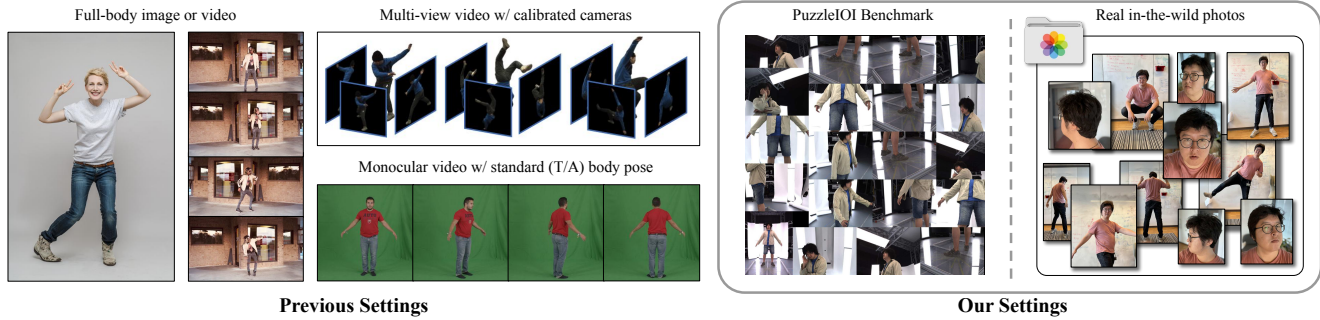


Fig. 2. **Image settings for avatar creation.** Past work (left) requires images with full-body visibility, known camera calibration, or simple human poses. Our PuzzleAvatar method operates on in-the-wild photos (right); it assumes a consistent outfit, hairstyle and accessories, but deals with unconstrained human poses, camera settings, lighting and background). Our PuzzleIOI dataset contains multi-view images with challenging crops paired with 3D ground truth.

2023; Ma et al. 2020; Shen et al. 2023; Xiong et al. 2024; Yu et al. 2021; Zheng et al. 2019], in which full human bodies in limited body poses are captured using well calibrated and synchronized cameras with controlled lighting and simple backgrounds; see Fig. 2.

While it is possible to create avatars from monocular (image or video) input as shown by some methods [Habermann et al. 2020; Xiu et al. 2022; Yang et al. 2023], such methods perform poorly for unusual body poses, motion blur, and occlusions, because they rely on accurate human and camera pose estimation from full-body shots. Instead, we bypass pose estimation, and follow the new paradigm of “reconstruction as conditional generation”, as recently demonstrated for Text-to-Image (T2I) generation [Gao et al. 2023; Huang et al. 2024b; Wu et al. 2024; Yang et al. 2024; Zhang et al. 2023]. Specifically, these works cast reconstruction from partial observations as “inpainting” unobserved regions through foundational-model priors, while imposing cross-view consistency. We adapt existing T2I work [Avrahami et al. 2023] to learn **subject-specific** priors from a **personal OOTD** image collection, by finetuning T2I models on such images to capture identity, pieces of clothing, accessories, and hairstyle into unique and inter-exchangeable tokens, and extracting 3D geometry and texture with Score Distillation Sampling (SDS) based techniques [Poole et al. 2023]. Metaphorically, our model swallows relatively “unstructured” data and digests this into a “structured library”; that is, “seeking order in chaos, finding harmony in turmoil.”

Our insight to treat T2I models as personalized priors enables us to not only avoid *explicit* per-pixel correspondences to a canonical human space, but also to build avatars in a compositional manner. To this end, given a photo collection of a person, various assets are extracted via an open-vocabulary segmentor [Ren et al. 2024], such as the face, garments, accessories, and hairstyles. Each of these assets is labeled by a unique token as “<asset X>”. We exploit these token-asset pairs, to finetune a pre-trained T2I model, so that it learns to generate “personalized” assets given a respective token. Based on this personalized T2I model, we produce a 3D human avatar via Score Distillation Sampling (SDS) given a descriptive and compositional text prompt, e.g., “a DSLR photo of a man, with <asset1> face, wearing <asset0> shirt, ...” (see Fig. 1). Here, each unique asset is like a puzzle piece, characterizing the identity, hairstyle and dressing style of the person. In a sense, the

learned tokens are used as puzzle pieces to assemble avatars, guided by text prompts. Thus, we call our method “**PuzzleAvatar**”.

Since there exists no benchmark for our new **Album2Human** task, we collect a new dataset, called PuzzleIOI, of 41 subjects in a total of roughly 1k configurations (outfits, accessories, hairstyles). Our evaluation metrics include both *3D reconstruction errors* (e.g., Chamfer distances, P2S distances) between reconstructed shapes and ground-truth 3D scans, as well as *2D image similarity measures* (e.g., PSNR, SSIM) between rendered multi-view images of the reconstructed surface and ground-truth textured scans. Our PuzzleAvatar is compatible with different types of diffusion models. We evaluate this on PuzzleIOI using two diffusion models, namely single-view Stable Diffusion [Rombach et al. 2022] and multi-view MVDream [Shi et al. 2024]. Moreover, we evaluate the contribution of each model component both qualitatively and quantitatively with an in-depth ablation analysis (Section 4.4).

In summary, here we make the following main contributions:

Task: We introduce a novel task, called “Album2Human”, for reconstructing a 3D avatar from a personal photo album with a consistent outfit, hairstyle and accessories, but unconstrained human pose, camera settings, framing, lighting and background.

Benchmark: For evaluation of our novel task, we collect a new dataset, called PuzzleIOI, with challenging cropped images and paired 3D ground truth. This facilitates quantitatively evaluating methods on both 3D reconstruction and view-synthesis quality.

Methodology: PuzzleAvatar follows the fresh paradigm of “reconstruction as conditional generation”, that is, it performs implicit human canonicalization using a personalized T2I model to bypass explicit pose estimation, or re-projection pixel losses.

Analysis: We conduct detailed evaluation and ablation studies to analyze the effectiveness and scalability of PuzzleAvatar and each of its components, shedding light on potential future directions.

Downstream applications: We show that PuzzleAvatar’s highly-modular tokens and text guidance facilitates downstream tasks through two examples: character editing and virtual try-on.

Please check out more qualitative results and demos of applications in [video](#). PuzzleAvatar is a step towards personalizing 3D avatars. To democratize this, code and PuzzleIOI dataset will be made public for only research purpose.

2 RELATED WORK

3D Human Creation. Many works have explored how to reconstruct clothed humans from visual cues like multi-view images [Lin et al. 2024; Peng et al. 2023; Saito et al. 2019] or full-shot monocular video [Alldieck et al. 2018a,b; Li et al. 2020; Weng et al. 2022]. Recently, a lot of works strive to create human avatars characterized by language. Initial work guided by language uses a CLIP embedding [Hong et al. 2022] to sculpt coarse body shape. Recent work [Cao et al. 2024; Huang et al. 2023a; Kolotouros et al. 2023; Liao et al. 2024; Wang et al. 2023b] captures finer geometry and texture for a clothed human, or multiple humans, by exploiting large-scale text-to-image models and Score Distillation Sampling (SDS) [Poole et al. 2023; Wang et al. 2023a]. In addition to text, when subject images are available, they are used to finetune the pretrained model [Ruiz et al. 2023] and to encourage fidelity via re-projection losses [Gao et al. 2023; Huang et al. 2023b, 2024b; Yang et al. 2024]. While SDS frameworks typically take a few thousand iterations, other work [Chen et al. 2024] speeds up the process by one-step generation conditioned on a given image input. However, all image-conditioned methods assume reliable human pose estimation [Pavlakos et al. 2019] as a proxy representation to draw correspondences between the input image and the reconstructed 3D avatar. Hence, they require images with clean backgrounds, common body poses, and full-body views without crops. Furthermore, external controllers (e.g., ControlNet [Zhang and Agrawala 2023], Zero123 [Liu et al. 2023]) and additional geometric regularizers (e.g., Laplacian and Eikonal [Chen et al. 2023]) appear essential to achieve high-quality output. In contrast, PuzzleAvatar does not require any of these, thus, it is uniquely capable of operating on unconstrained personal-album photos.

Pose-Free Reconstruction in the wild. In our work, the term “pose” refers not only to camera pose but also to body articulation. Camera pose plays a crucial role in 3D reconstruction, as it “anchors” 3D geometry onto 2D images [Mildenhall et al. 2021], however, estimating it for in-the-wild images is highly challenging. Thus, to account for camera estimation errors, some work leverages joint optimization between the object and camera [Lin et al. 2021; Wang et al. 2021; Xia et al. 2022], off-the-shelf geometric cue estimates [Bian et al. 2023; Fu et al. 2024a; Meuleman et al. 2023], or learning-based camera estimation [Wang et al. 2024c,b; Zhang et al. 2024]. Body pose is also hard to estimate from in-the-wild images and is much higher dimensional than camera pose. Some work can reconstruct static scenes from in-the-wild images with challenging illumination conditions and backgrounds [Martin-Brualla et al. 2021; Sun et al. 2022], but these cannot be applied to articulated objects, like humans. In our work, we tackle all above challenges for “pose-free” human reconstruction. That is, we tackle in-the-wild photos with unknown camera poses, unknown body poses, possibly truncated images (e.g. headshots), and diverse backgrounds and illumination conditions, which are highly challenging for existing methods.

Large Vision-Language Models. Large foundation models have achieved great progress in visual understanding [Kirillov et al. 2023; Li et al. 2022; Radford et al. 2021] and generation [Athanasiou et al. 2023; Brooks et al. 2024; Rombach et al. 2022]. As they are trained on a tremendous amount of data, their strong generalizability can

be exploited for downstream tasks. In particular, Score-Distillation-Sampling techniques stand out [Poole et al. 2023; Wang et al. 2023a] for distilling “common knowledge” from text-to-image models towards creating 3D objects. Work on model customization injects new concepts via fine-tuning (partial or whole) pre-trained networks [Avrahami et al. 2023; Jain et al. 2022; Kumari et al. 2023; Liu et al. 2024b; Ruiz et al. 2023]. Other work re-purposes the diffusion models to new tasks [Fu et al. 2024b; Ke et al. 2024; Kocsis et al. 2024]. We leverage all the above techniques for faithful 3D human-avatar generation from natural images, a challenging task involving widely varying appearance, lighting, backgrounds, body and camera poses.

3 METHOD

Given an image collection $\{I_1, I_2, \dots, I_N\}$ of a person, we aim to build a 3D avatar that captures the person’s shape ψ_g and appearance ψ_c . Notably, personal daily-life photos are unconstrained (see Fig. 2) as humans (1) appear in diverse poses and scales, (2) are often occluded or largely truncated, and (3) are captured from unknown viewpoints in diverse backgrounds. Thus, camera calibration and pose canonicalization for these photos are extremely challenging, making direct reconstruction of human avatars difficult.

Our key insight is to circumvent estimating human body poses and cameras, and, instead, to perform implicit human canonicalization via a foundation vision-language model (e.g., Stable Diffusion [Rombach et al. 2022]). Our method is summarized visually in Fig. 3, and has two main stages. Specifically, we first “decompose” photos into multiple assets (e.g., garments, accessories, faces, hair), all of which are linked with unique learned tokens by a personalized T2I model, PuzzleBooth (Sec. 3.1), that is G_{puzzle} in Fig. 3. Then, we “compose” these multiple assets into a 3D full-body representation ψ_g, ψ_c via Score Distillation Sampling (SDS) (Sec. 3.2).

3.1 PuzzleBooth – Personalize Puzzle Pieces

Our first step is to segment subject images into multiple assets representing different human parts such as trousers, shoes, and hairstyle. While one could build each asset individually, we adapt the “Break-A-Scene” [Avrahami et al. 2023], which shows that jointly learning multiple concepts significantly boosts performance, possibly because this facilitates global reasoning when multiple regions are simultaneously generated. Such a strategy is even more beneficial in our setting since human-related concepts, such as face and hair, are harder to learn as their properties are strongly correlated compared to clearly distinct objects in the setting of “Break-A-Scene.”

Asset Creation. All images are segmented into multiple assets V_k , each of which is associated with a segmentation mask \mathcal{M}_k , a dedicated learnable token $[v_k]$, and its textual name $[c_k]$, such as “pants” or “skirt.” In addition, we also obtain a coarse view direction d for each image. All such information is obtained automatically by Grounded-SAM [Ren et al. 2024] and GPT-4V [OpenAI 2023]. Specifically, we query GPT-4V with an image to directly get the property of each asset $[c_k]$ and coarse view direction d . Then, given the full list of queried asset names $\{[c_k]\}_{k=1}^K$, Grounded-SAM outputs segmentation masks if they are present. Please refer to Appendix A for our full prompt template.

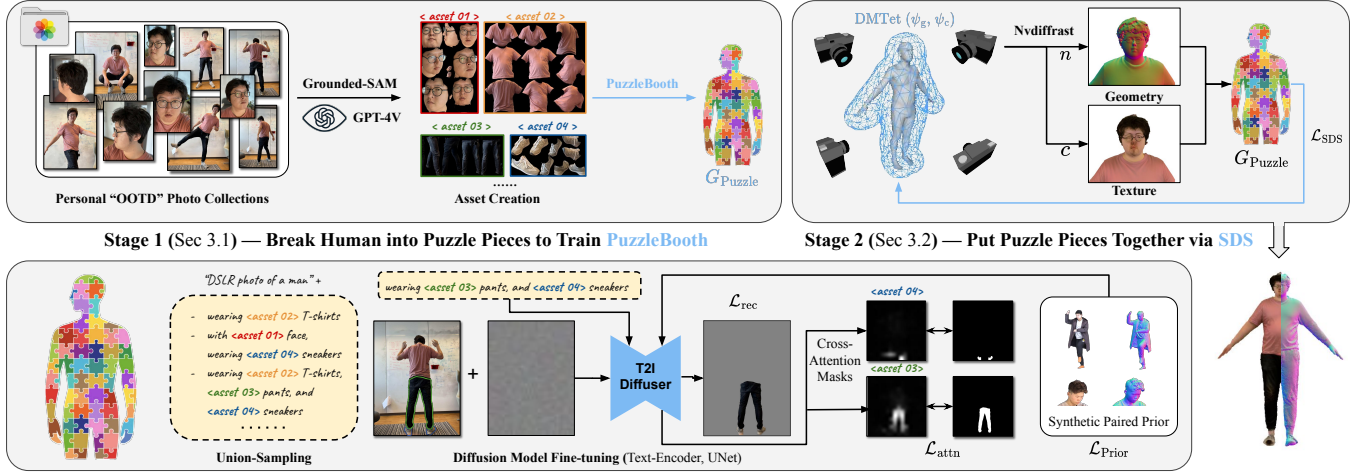


Fig. 3. **Overview of PuzzleAvatar.** The upper figure shows the two main stages: (1) *PuzzleBooth* (Section 3.1), where the unconstrained photo collections are captioned and segmented to create personalized puzzle pieces, for training *PuzzleBooth*, G_{puzzle} , and (2) *Create-3D-Avatar* (Section 3.2), where the T-posed textured tetrahedral body mesh is optimized using a multi-view SDS loss \mathcal{L}_{SDS} . The bottom figure illustrates the training details of *PuzzleBooth*; the Text-Encoder and the UNet of T2I Diffuser (i.e., Stable Diffusion) are fine-tuned using the masked diffusion loss, \mathcal{L}_{rec} (Eq. (1)), cross-attention loss, $\mathcal{L}_{\text{attn}}$ (Eq. (2)), and prior preservation loss, $\mathcal{L}_{\text{prior}}$ (Eq. (3)). Components marked in light blue are trainable or optimizable.

Two-Stage Personalization. We finetune the pretrained text-to-image diffusion model [Rombach et al. 2022; Shi et al. 2024] so that it adapts to the new assets. Following “Break-A-Scene” [Avrahami et al. 2023], we optimize the “text” part, i.e., the text embedding of asset token $[v_j]$, and the “visual” part, i.e., the weights of the diffusion model, in two stages: In the first stage, only text embeddings of the asset tokens $[v_k]$ are optimized with a large learning rate. In the second stage, both the “text” and “visual” part are optimized with a small learning rate. This strategy effectively prevents guidance collapse [Gao et al. 2024] between newly introduced tokens $[v_k]$ and existing asset names $[c_k]$, or, equivalently, preserves the compositionality of visual concepts.

During training, we randomly select, for every image I , a subset of assets that appear in the image and train the model on the union set of these selected assets. This union sampling strategy, originally introduced in [Avrahami et al. 2023], is crucial for effective asset disentanglement. Specifically, the *mask union* is done via a pixel-wise union operation $\mathcal{M}_U = \cup_{i=1}^j \mathcal{M}_i$, while the *image union* applies the union mask on the image, $\mathcal{I}_U = I \odot \mathcal{M}_U$. The union text prompt p_U is constructed by concatenating selected assets, i.e. “a high-resolution DSLR colored image of a man/woman with $[v_1]$ $[c_1]$, ..., $[v_2]$ $[c_2]$, and wearing $[v_3]$ $[c_3]$, ..., $[v_j]$ $[c_j]$, $[d]$ view”.

Losses. In both optimization stages, the model is trained to encourage concept separation while still retaining its generalization capability. To do so, the model is optimized with three loss terms: a Masked Diffusion Loss, \mathcal{L}_{rec} , Cross-Attention Loss, $\mathcal{L}_{\text{attn}}$, and Prior Preservation Loss, $\mathcal{L}_{\text{prior}}$. The overall training objective is $\mathcal{L}_{\text{total}} = \mathcal{L}_{\text{rec}} + \lambda_{\text{attn}} \mathcal{L}_{\text{attn}} + \mathcal{L}_{\text{prior}}$ where $\lambda_{\text{attn}} = 0.01$.

The *Masked Diffusion Loss* encourages fidelity in replicating each concept via a pixel-wise reconstruction within the segmented mask:

$$\mathcal{L}_{\text{rec}} = \mathbb{E}_{z, \epsilon \sim \mathcal{N}(0,1), t} [\|[\epsilon - \epsilon_{\theta}(z_t, t, p_U)] \odot \mathcal{M}_U\|_2^2], \quad (1)$$

where \mathcal{M}_U is the union mask, and $\epsilon_{\theta}(z_t, t, p_U)$ is the denoised output at diffusion step t given the union prompt, p_U .

To disentangle different learned assets, we use a *Cross-Attention Loss* [Avrahami et al. 2023] to encourage each of the newly-added tokens to be exclusively associated with only the target asset:

$$\mathcal{L}_{\text{attn}} = \mathbb{E}_{z, j, t} [\|C\mathcal{A}_{\theta}(v_j, z_t) - \mathcal{M}_j\|_2^2], \quad (2)$$

where $C\mathcal{A}_{\theta}(v_j, z_t)$ is the cross-attention map in the diffusion U-Net between the newly-added token, $[v_j]$, and the visual feature, z_t .

Lastly, we apply a *Prior Preservation Loss* [Ruiz et al. 2023] to retain the generalization capability of the vanilla T2I model – Stable Diffusion (SD-2.1). The model is trained to reconstruct images with general concepts when the special tokens are removed from prompts. General human images come from two sources: (1) Generated images, $\mathcal{I}_{\text{gen}}^{\text{pr}}$, come from SD. (2) Synthetic color-normal pairs (see Fig. 4), $\mathcal{I}_{\text{syn}}^{\text{pr}}$, rendered from multiple views, come from THuman2.0 [Yu et al. 2021]. The latter is to improve the geometry quality and color-normal consistency [Huang et al. 2024a]. Instead of applying prior preservation loss for individual concepts separately, we find it beneficial to compute the loss on the entire human images.

$$\mathcal{L}_{\text{prior}} = \mathbb{E}_{z^{\text{pr}}, \epsilon \sim \mathcal{N}(0,1), t} [\|[\epsilon - \epsilon_{\theta}(z_t^{\text{pr}}, t, p_U^*)]\|_2^2] \quad (3)$$

where p_U^* is the text prompt without special tokens.

3.2 PuzzleAvatar – Put Puzzle Pieces Together

With the fine-tuned diffusion model customized for all provided assets, we are able to distill a descriptive 3D avatar via SDS.

Score Distillation Sampling (SDS). A pretrained diffusion model over images $D(z)$ captures the data distribution $\log p(z_{\psi})$. SDS [Poole et al. 2023] is a technique that guides some parameterization of images $z(\psi)$ (raw pixels, neural networks, etc.) to generate

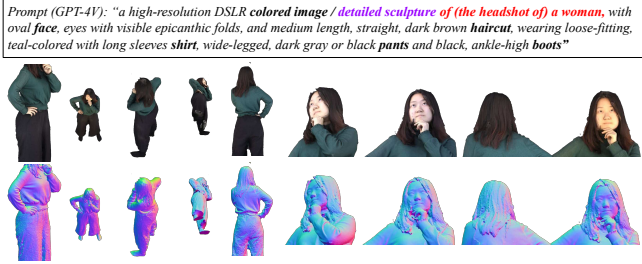


Fig. 4. **Color-Normal Synthetic Prior.** The corresponding descriptions are generated via GPT-4V [OpenAI 2023], where the prompt of RGB image starts with “a high-resolution DSLR colored image”, while that of the normal image starts with “a detailed sculpture of”. The zoom-in head images are generated by appending “the headshot of”

images towards higher likelihood. The core idea is to approximate the parameter gradient $\nabla_{\psi} \mathcal{L}$ as a weighted reconstruction residual. As the vanilla method suffers from color oversaturation, we use an improved SDS – Noise-Free Distillation Sampling (NFDS) [Katzir et al. 2024]. This modifies the guidance from a single reconstruction residual into two composed residual terms δ_C and δ_D . Specifically, by denoting the derived gradient of a network ψ from NFSD as $\nabla \mathcal{L}_{\text{NFDS}}[x, \psi]$:

$$\nabla_{\psi} \mathcal{L}_{\text{NFDS}}[z, \psi] = w(t)(\delta_D + s\delta_C) \frac{\partial z}{\partial \psi}, \quad \text{where} \quad (4)$$

$$\delta_C(z_t, p, t) = \epsilon_{\theta}(z_t; p, t) - \epsilon_{\theta}(z_t; \emptyset, t),$$

$$\delta_D(z_t, t) = \begin{cases} \epsilon_{\theta}(z_t; \emptyset, t), & \text{if } t \leq 200 \\ \epsilon_{\theta}(z_t; \emptyset, t) - \epsilon_{\theta}(z_t; p^{\text{neg}}, t), & \text{otherwise,} \end{cases} \quad (5)$$

In our case, z is the (latent of) diffusion output (human images or normals) and ψ denotes the 3D avatar representation (both ψ_g, ψ_c), s is the guidance scale, we follow NFDS and set $s = 7.5$.

Representation and Initialization. The 3D human avatar is parameterized with DM Tet [Gao et al. 2020; Shen et al. 2021], a flexible tetrahedron-based 3D neural representation. The geometry, ψ_g , and appearance, ψ_c , are optimizable, and can be differentially rendered into normal, n , and colored images, c . The geometry ψ_g is first initialized to an A-posed SMPL-X body [Pavlakos et al. 2019].

Optimization. We use the full-text description of the human p^{all} as a guiding prompt. It is a concatenation of text prompts from all assets i.e., $(v_i, c_i), \dots, (v_K, c_K)$. We optimize geometry and color separately in two optimization stages, both using Noise-Free-Score Distillation (NFSD). In the first stage, the avatar’s geometry is guided in the surface normal space, $\nabla \mathcal{L}^{\text{norm}} \equiv \nabla \mathcal{L}_{\text{NFDS}}[n, \psi_g]$. We additionally prepend “a detailed sculpture of” to the full-text to indicate the guidance space. In the second stage, its appearance is guided by $\nabla \mathcal{L}^{\text{color}} \equiv \nabla \mathcal{L}_{\text{NFDS}}[c, \psi_c]$. The camera settings for multi-view SDS are in Appendix B.

4 EXPERIMENTS

It has been a long-standing challenge in the field of “Text-to-3D” (including “Text-to-Avatar”) to *quantitatively* benchmark new algorithms. Existing benchmarks are typically less reliable because

Table 1. **Datasets related to PuzzleIOI.** “–” means image captures are unavailable. “Scan” is A-posed, and “SMPL-X” is its respective SMPL-X fits.

Dataset	Reference	#Views	#ID	#Outfits	#Actions	SMPL-X	Scan	Text	Texture
ActorsHQ	[Isgk et al. 2023]	160	8	8	52	✓	✓	✗	✓
MVHumanNet	[Xiong et al. 2024]	48	4500	9000	500	✓	✗	✓	✓
HuMMan	[Cai et al. 2022]	10	1000	1000	500	✗	✗	✗	✓
DNA-Rendering	[Cheng et al. 2023]	60	500	1500	1187	✗	✗	✗	✓
THuman2.0	[Yu et al. 2021]	–	200	500	–	✗	✗	✗	✓
CAPE	[Ma et al. 2020]	–	15	8	600	✓	✓	✗	✗
BUFF	[Zhang et al. 2017]	–	5	2	3	✓	✓	✗	✓
PuzzleIOI (Ours)		22	41	933	40	✓	✓	✓	✓

they sample 3D avatars from a relatively small collection of prompts and evaluate the quality of these avatars through perceptual studies with a limited number of participants.

While PuzzleAvatar adopts “Text-to-3D” techniques, its goal is to reconstruct avatars from photos of a specific person in a specific outfit, rather than to randomly generate avatars. As a result, a natural and reliable way to benchmark PuzzleAvatar is to exploit a 4D scanners (synced with IOI color cameras¹) for capturing ground-truth 3D shape and appearance, and to measure the reconstruction error between the reconstructed and ground-truth shape and appearance. We thus build a dataset, called PuzzleIOI (Section 4.1), on which we evaluate PuzzleAvatar and ablate its components.

4.1 PuzzleIOI Dataset

We create PuzzleIOI (see statistics in Table 1) to simulate real-world album photos of humans, which: (1) cover a wide range of human identities (#ID column in Table 1) and daily outfits (#Outfits), (2) span numerous views (#Views) to mimic real-world captures (e.g., occlusion, out-of-frame cropping), and (3) include text descriptions (Text), and ground-truth textured A-posed scans (Scan, Texture) and their SMPL-X fits (SMPL-X) for shape initialization purposes.

A-Pose SMPL-X & Scan. Almost all “Text-to-Avatar” methods [Cao et al. 2024; Huang et al. 2024a; Kolotouros et al. 2023; Liao et al. 2024; Yuan et al. 2023] use an A-pose body for shape initialization due to its minimal self-occlusions. Thus, we adhere to this empirical setting in PuzzleIOI. For each subject (ID+Outfit), we capture a ground-truth A-posed 3D scan and fit a SMPL-X model to it, as in AGORA [Patel et al. 2021].

Multiple Views. To simulate the diversity and imperfections of real-world photos, for each subject (ID+outfit) we randomly sample 120 photos from the multi-view human action sequence (approx. 760 frames / subject) captured by 22 cameras; see Fig. 2. The captured images are segmented and shuffled to build the training dataset for PuzzleBooth (Section 3.1).

Text Description. Similar to how image captioning is done in Section 3.1, here we randomly select two frontal full-body images and use GPT-4V to query the asset names and corresponding descriptions of visible assets. We use the position of the ground truth camera to categorize the photos into 4 view groups {front, back, side, overhead} in PuzzleIOI, while we use GPT-4V to automatically label viewpoints from in-the-wild images.

¹<https://www.ioindustries.com/cameras>

4.2 2D and 3D Metrics

We conduct quantitative evaluation on the PuzzleIOI dataset (Sec. 4.1). To evaluate the quality of **shape reconstruction** we report three metrics: (1) **Chamfer distance** (bidirectional point-to-surface, *cm* as unit), (2) **P2S distance** (1-directional point-to-surface, *cm* as unit) distance, and (3) **L2 error for Normal maps** rendered for four views ($\{0^\circ, 90^\circ, 180^\circ, 270^\circ\}$) to capture local surface details.

To evaluate the quality of **appearance reconstruction**, we render multi-view color images as above, and report three image-quality metrics: **PSNR** (Peak Signal-to-Noise Ratio), **SSIM** (Structural Similarity) and **LPIPS** (Learned Perceptual Image Path Similarity).

4.3 Benchmark

PuzzleAvatar is a general framework, compatible with different diffusion models. In Table 2 we benchmark variants of PuzzleAvatar with two different backbones: (1) vanilla Stable Diffusion [Rom-bach et al. 2022], i.e., SD-2.1², and (2) MVDream [Shi et al. 2024]³ fine-tuned from vanilla SD using multi-view images rendered from Objaverse [Deitke et al. 2023]. The shared basic pipeline for our PuzzleAvatar, the state-of-the-art image-to-3D methods TeCH [Huang et al. 2024b] and MVDreamBooth [Shi et al. 2024] is: 1) first to finetune these backbones with subject images and 2) later to extract avatars with text-guided SDS optimization.

Quantitative Evaluation. Table 2 shows that PuzzleAvatar is on par with TeCH on 3D metrics, while outperforming it on all 2D metrics. Note that, to enhance shape quality, TeCH employs multiple supervision signals and regularization terms, including normal maps predicted from the input image via ECON [Xiu et al. 2023], silhouette masks produced by SegFormer [Xie et al. 2021] and a Laplacian regularizer. In terms of texture quality, TeCH uses an RGB-based chamfer loss to minimize color shift between the input image and the backside texture, while its front-side texture is achieved by back-projecting the input image. In contrast, PuzzleAvatar achieves on-par 3D accuracy and better texture quality *without* any of these auxiliary losses, regularizers, or pixel back-projection.

As for the MVDream-based comparison, PuzzleAvatar outperforms MVDreamBooth on texture quality by a large margin (PSNR +10.09%, LPIPS -8.79%), and on geometry quality (measured by Chamfer and P2S), while showing comparative performance with the baselines on normal consistency. The key difference of PuzzleAvatar, compared to MVDreamBooth and TeCH, is its puzzle-wise training strategy. Without this, 2D diffusion models fine-tuned on human photos with complex poses and cropping might produce completely flawed 3D humans, with low-quality (even full black) textures or overly smooth shapes; see Fig. 7.

Qualitative Evaluation. As depicted in Fig. 7, PuzzleAvatar has various advantages over TeCH: (1) *Enhanced front-back consistency*, because PuzzleAvatar treat all views with ID-consistent generation, while TeCH introduces inconsistency between the front view created by reconstruction and the back view created by imagination. (2) *Reduced non-human artifacts*, PuzzleAvatar bypass the dependence on numerous off-the-shelf estimators used in TeCH, for which

non-human artifacts arise when segmentation or normal map estimation fails. (3) *Improved geometry-texture disentanglement*, where PuzzleAvatar excels in separating shirt stripes compared to TeCH. This mainly attributes to the failed normal map estimated from the input image (see Fig. 7 3th row, rightmost normal estimate), which relies on often incorrectly estimated normal maps from the input image. Notably, MVDreamBooth highlights PuzzleAvatar’s proficiency in producing intricate geometric details and textures. We also compare with AvatarBooth [Zeng et al. 2023], which addresses the similar problem. Since its code and trained models have not been released yet, we test PuzzleAvatar on the same photo collections used by AvatarBooth, and show the results in Fig. 10 and [video](#).

4.4 Ablations

Ablation: Common Practices. In Table 3-B, we analyze the effect of common practices that have been shown to be beneficial for general scenes, including view-specific prompt [Ruiz et al. 2023], NFSD over vanilla SDS [Katzir et al. 2024], and prior preservation loss [Huang et al. 2024a; Ruiz et al. 2023]. The performance gain confirms that our problem also benefits from these practices. Some qualitative comparisons are shown in Figs. 8 and 9. Our ablation results show the effectiveness of PuzzleIOI metrics in measuring the performance of different methods in our setting, and also help us answer the following questions.

Does the view prompt $[d]$ helps the reconstruction? Yes. This is a common practice of numerous existing works [Chen et al. 2023; Huang et al. 2024b; Liao et al. 2024; Poole et al. 2023], and has not yet been quantitatively justified. As detailed in Table 3 (B. w/o view prompt), the normal error increased by +9.3%. Apart from view prompts captioned by LLM, there is still room to grow with improved representatives for cameras, such as camera pose embedding used in LGM [Tang et al. 2024] and Cameras-as-Rays [Zhang et al. 2024].

Does NSFD outperforms vanilla SDS? Yes. For fair comparison, we set the guidance scale $s = 7.5$ for both NSFD and vanilla SDS. As detailed in Table 3 (B. w/o NFSD), compared with NFSD (Noise-Free Score Distillation [Katzir et al. 2024]), vanilla SDS degrades the geometry quality a bit by +2.2%, while considerably degrading the texture quality (PSNR +17.3%, LPIPS +16.4%), as the SDS often crashes, leading to full-gray/yellow textures.

Does the synthetic human prior helps? Yes, and it significantly improves the reconstruction quality, in both the geometry (chamfer error -38.1%, P2S error -58.8%, Normal error -73.3%), and texture (PSNR +11.2%, LPIPS -27.9%). And synthetic normals appear to contribute more than synthetic RGB (chamfer error -31.5% vs. -5.7%, LPIPS -21.3% vs. -3.3%). Introducing photorealistic synthetic data during fine-tuning proves beneficial, and the performance boost from color-normal pairs surpasses that from only using single mode (color/normal) of data, such as chamfer (+38.1% > +31.5% + +5.7%) and LPIPS (+27.9% > +21.3% + +3.3%), see Fig. 5, we attribute such “**1+1>2 effect**” to the enhanced geometry-texture alignment, which benefits from such pairwise training. Please check out Fig. 8 for more qualitative ablation results.

Can token $[v_i]$ encode the identity and features of assets? Yes. As shown in Table 3 (A. w/ detailed GPT-4V description), both

²huggingface.co/stabilityai/stable-diffusion-2-1-base

³huggingface.co/ashawkey/mvdream-sd2.1-diffusers

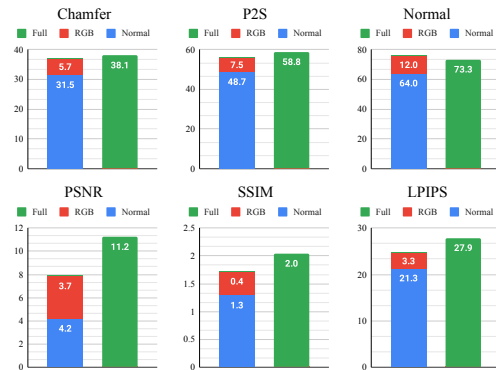
Table 2. **Evaluation on full PuzzleIOI (933 OOTD)**. † means using SMPL-X fits of ground-truth scans to initialize DM Tet and factor out pose error (unlike the vanilla TeCH [Huang et al. 2024b] that estimates SMPL-X using PIXIE [Feng et al. 2021]). The best results are marked with “**bold**”. “Ratio%” is the relative performance drop, while “ratio%” is the relative performance gain, w.r.t. the competitors, i.e. TeCH and MVDreamBooth [Shi et al. 2024].

Method	Backbone	3D Metrics (Shape)			2D Metrics (Color)		
		Chamfer ↓	P2S ↓	Normal ↓	PSNR ↑	SSIM ↑	LPIPS ↓
TeCH†	SD-2.1-base	1.646	1.590	0.076	23.635	0.919	0.065
PuzzleAvatar	SD-2.1-base	1.617 -1.76%	1.613 +1.45%	0.077 +1.32%	24.687 +4.45%	0.930 +1.20%	0.062 -4.62%
MVDreamBooth†	MVDream	1.705	1.835	0.100	19.401	0.909	0.091
PuzzleAvatar	MVDream	1.697 -0.47%	1.811 -1.31%	0.101 +1.00%	21.361 +10.09%	0.906 -0.33%	0.083 -8.79%

Table 3. **Ablation study on subset of PuzzleIOI (120 OOTD)**. The best results are marked with “**bold**”, the second best results are marked with and underline. The “ratio%” is the relative performance drop, and “ratio%” is the relative performance gain, w.r.t. PuzzleAvatar, where the drop larger than 20% are marked with “**bold**”. Group-A summarizes the *failed attempts*, Group-B justifies the *key components*, and Group-C analyses the *scalability* of our method.

Group	Method	3D Metrics (Shape)			2D Metrics (Color)		
		Chamfer ↓	P2S ↓	Normal ↓	PSNR ↑	SSIM ↑	LPIPS ↓
	TeCH†	1.600	<u>1.541</u>	0.073	23.665	0.919	0.065
	PuzzleAvatar	<u>1.589</u>	1.570	0.075	<u>24.718</u>	0.931	0.061
A.	w/ detailed GPT-4V description	1.604 +0.9%	1.607 +2.4%	0.079 +5.3%	24.208 -2.1%	0.929 -0.2%	<u>0.062</u> +1.6%
	w/o view prompt	1.641 +3.3%	1.653 +5.3%	0.082 +9.3%	23.929 -3.2%	0.928 -0.3%	0.064 +4.9%
	w/o NFSD (vanilla SDS)	1.624 +2.2%	1.604 +2.2%	<u>0.072</u> -4.0%	20.441 -17.3%	0.923 -0.9%	0.071 +16.4%
B.	w/o synthetic normal+color	2.194 +38.1%	2.493 +58.8%	0.130 +73.3%	21.940 -11.2%	0.912 -2.0%	0.078 +27.9%
	w/o synthetic normal	2.089 +31.5%	2.335 +48.7%	0.123 +64.0%	23.684 -4.2%	0.919 -1.3%	0.074 +21.3%
	w/o synthetic color	1.680 +5.7%	1.687 +7.5%	0.084 +12.0%	23.813 -3.7%	0.927 -0.4%	0.063 +3.3%
C.	multi-subject training (5 subjects / model)	1.809 +13.8%	1.560 -0.6%	0.080 +6.7%	24.990 +1.1%	0.929 -0.2%	<u>0.062</u> +1.6%
	w/o full-body images	1.603 +0.9%	1.580 +0.6%	0.073 -2.7%	23.703 -4.1%	0.931 0.0%	<u>0.062</u> +1.6%
	50% training data	1.590 +0.1%	1.569 -0.1%	0.074 -1.3%	24.095 -2.5%	0.930 -0.1%	0.061 0.0%
	10% training data	1.583 -0.4%	1.531 -2.5%	0.069 -8.0%	23.477 -5.0%	0.928 -0.3%	0.062 +1.6%

Fig. 5. “1+1>2 Effect” of Synthetic Priors. All the numbers refer to the performance gain (%), where **Full** means training with color-normal pairs, and **RGB** and **Normal** means training with single modality.



shape and color quality slightly decrease when too-detailed descriptions are used in the prompt, such as “wearing sleeveless <asset1> t-shirts, and fitted <asset2> jeans”, instead of “wearing <asset1> t-shirts, and <asset2> jeans”. Surprisingly, more detailed prompts can introduce bias, conflicting with the original identity and harming performance; see Fig. 9.

Does PuzzleAvatar work without using any full-body shots? Yes but with some performance drop. Excluding the full-body shots

(i.e., complete images), slightly decreases the quality of both geometry and texture (Chamfer +0.9% and PSNR -4.1%; Table 3, C. w/o full-body images). Nevertheless, it is unsurprising to find that PuzzleAvatar without training on full-body images still outperforms the best TeCH setting (better texture plus on-par geometry quality).

How much data does PuzzleAvatar need? With just a fraction of the training data (10%), PuzzleAvatar can already achieve satisfactory reconstruction performance. As the number of training images increasing, the view synthesis performance initially keeps improving in both texture and geometry quality (shown in Table 3, C. 50% / 10% training data) but interestingly starts to deteriorate in geometry quality. We hypothesize that training PuzzleAvatar using more RGB images could impair the quality of SDS gradients in the space of normal maps, thus degrading the geometry optimized via SDS. We find some empirical evidence supporting this hypothesis Table 3 (B. without synthetic normal), where the absence of normal priors leads to a notable decline in geometry quality compared to texture (P2S +48.7% vs. SSIM -1.3%).

Does PuzzleAvatar support multi-subject training? Yes. In fact, and perhaps surprisingly, multi-subject training even slightly improves reconstruction quality (Table 3-C). This demonstrates the power of Stable Diffusion to process and integrate numerous human identities simultaneously, and the robustness of our puzzle-based training strategy in learning disentangled human identities.

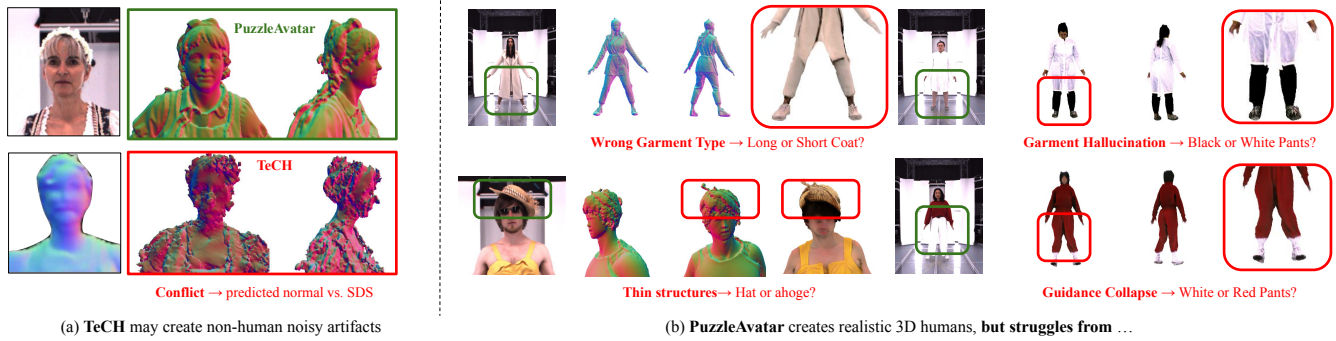


Fig. 6. **Failure Cases.** Non-human artifacts mainly cause errors in TeCH (see a), whereas errors in PuzzleAvatar stem from hallucination and flawed DMTet modeling of thin structures. For the right-top case, the black pants showing through the white coat, while realistic, deviates from the original input. As a result of this hallucination, the failures of PuzzleAvatar are distinct from ground-truth, but not completely catastrophic (see b).

5 APPLICATIONS

The compositionality of PuzzleAvatar through its tokens and text prompts supports diverse applications like Virtual Try-On and text-guided avatar editing, as shown in Fig. 1 and video. Moreover, the A-Posed output can simplify the rigging and skinning process. With the underlying SMPL-X parametric body, the 3D output could be easily animated with SMPL-X motion data, like AMASS [Mahmood et al. 2019] and AIST++ [Li et al. 2021], as the common practice in [Huang et al. 2020; Xiu et al. 2022; Zheng et al. 2021].

6 CONCLUSION

Limitations & Future Work. Since PuzzleAvatar builds on PuzzleBooth and Score Distillation Sampling (SDS), while using no re-projection terms, some hallucination is inevitable. As Fig. 6 shows, PuzzleAvatar may incorrectly hallucinate garment texture or types, and suffer from description contamination, a common issue in T2I models. Despite being trained with synthetic paired data, our model sometimes struggles to perfectly disentangle shape and color, leading to baked-in texture. Additionally, preserving facial identity is challenging without high-resolution headshot selfies in the training data. Potential solutions for better identity preservation may include enhancing segmented faces with super-resolution techniques [Wang et al. 2022], conducting personalized restoration [Chari et al. 2023], or incorporating face ID embeddings [Wang et al. 2024a].

PuzzleAvatar’s main issue currently is its computational complexity, as spending roughly 4 hours to train PuzzleBooth and perform SDS-based optimization is impractical for certain applications. In the future we will explore better training-free strategies [Li et al. 2024; Tewel et al. 2024] and better sampling methods for diffusion models [Luo et al. 2023; Song et al. 2023]. Besides, the compositional 3D could be achieved through non-watertight and multi-layer representations [Feng et al. 2022; Liu et al. 2024a; Son et al. 2024].

Multi-subject training with PuzzleAvatar seems promising. Thus, it might be feasible to extend PuzzleAvatar to decentralized training settings. By fine-tuning a shared T2I model through federated learning [Liangze and Lin 2023], users across the globe could upload their personal albums to build a global “style set” of really diverse clothing, accessories, and hairstyles, for customizing avatars.

Potential Negative Effect. As discussed in Sec. 4.4, the performance of PuzzleAvatar relies heavily on existing public/commercial synthetic datasets and therefore may inherit their gender, racial and age biases. One may address such an issue by curating balanced datasets from real-world images (with off-the-shelf methods to estimate normals [Bae and Davison 2024; Saito et al. 2020; Xiu et al. 2023, 2022]) or by simply building better synthetic datasets.

Contributions to the Community. PuzzleAvatar paves the way in reconstructing articulated humans from personal, natural photo collections – introducing the new “Album2Human” task. Meanwhile, PuzzleIOI offers a new benchmark that facilitates *objective* evaluation of various diffusion-model-based techniques, including but not limited to model customization, model personalization and distillation sampling. We believe that our new task, Album2Human, together with our new benchmark, PuzzleIOI, could push the boundary of the field of AI-Generated Content (AIGC). Furthermore, PuzzleAvatar offers a simple yet scalable reconstruction system, with which users may ignore the technical details of reconstruction parameters. More importantly, we believe that PuzzleAvatar demonstrates a new and practical paradigm for “*puzzle-assembled clothed human reconstruction*” that produces a 3D avatar from everyday photos in a scalable and constraint-free manner.

Acknowledgments. We thank Peter Kulits and Yandong Wen for proofreading, Yifei Zeng for providing the results of AvatarBooth, Yamei Chen and Kexin Wang for teaser photos, Jiaxiang Tang, Yangyi Huang, Nikos Athanasiou, Yao Feng and Weiyang Liu for fruitful discussions, Jinlong Yang and Tsvetelina Alexiadis for data capture. This project has received funding from the European Union’s Horizon 2020 research and innovation programme under the Marie Skłodowska-Curie grant agreement No.860768 (CLIFE project). Yufei Ye’s PhD research is partially supported by a Google Gift.

Disclosure. MJB has received research gift funds from Adobe, Intel, Nvidia, Meta/Facebook, and Amazon. MJB has financial interests in Amazon and Meshcapade GmbH. While MJB is a co-founder and Chief Scientist at Meshcapade, his research in this project was performed solely at, and funded solely by, the Max Planck Society.

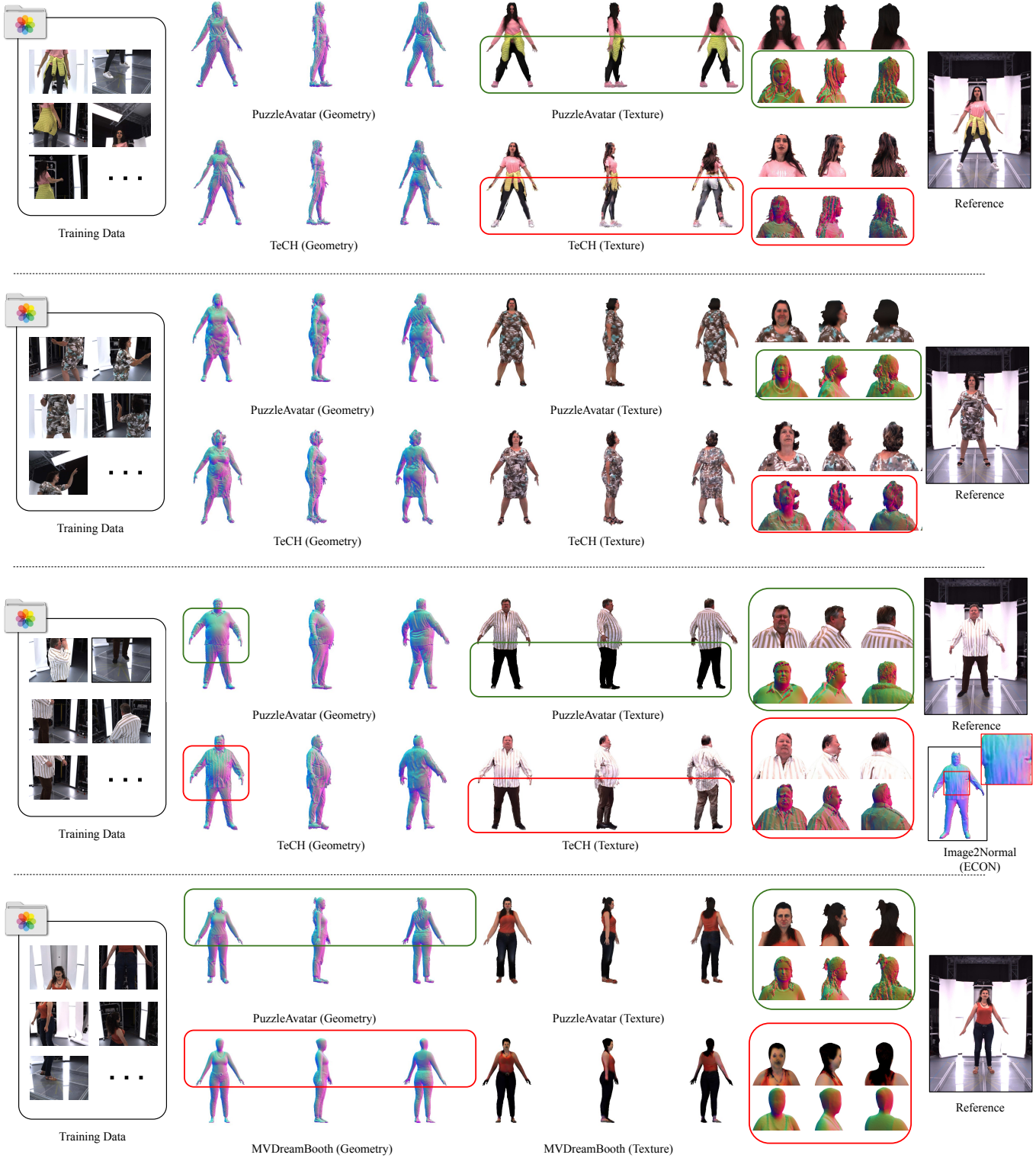
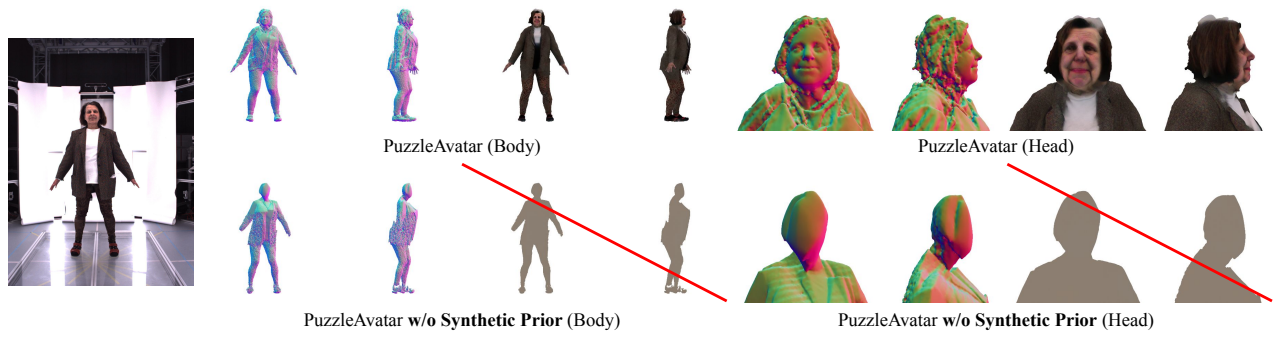
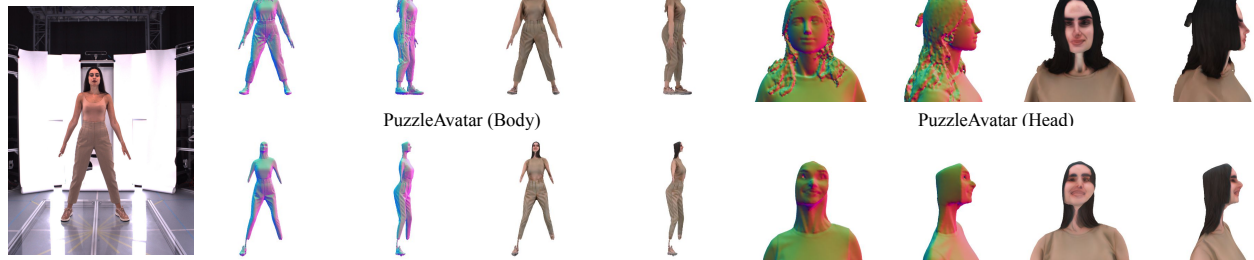


Fig. 7. **Qualitative Results.** We compare PuzzleAvatar, TeCH and MVDreamBooth on randomly sampled subjects. PuzzleAvatar offers various advantages over TeCH: (1) Enhanced front-back consistency. (2) Reduced non-human artifacts. (3) Improved geometry-texture disentanglement. At the bottom, MVDreamBooth highlights PuzzleAvatar’s proficiency in producing intricate geometric details and textures. **Q Zoom in** to see more 3D and color details.



PuzzleAvatar w/o Synthetic Prior (Body)

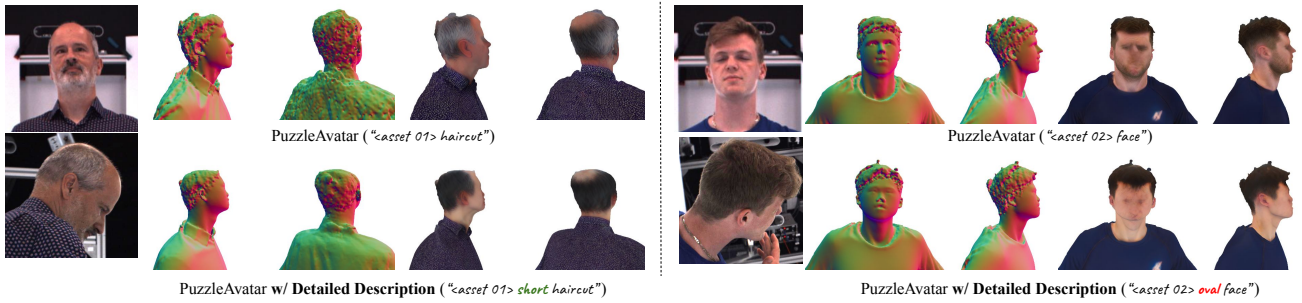
PuzzleAvatar w/o Synthetic Prior (Head)



PuzzleAvatar w/o Synthetic Prior (Body)

PuzzleAvatar w/o Synthetic Prior (Head)

Fig. 8. **How Synthetic Prior Helps?** See Fig. 5 for more in-depth analysis.



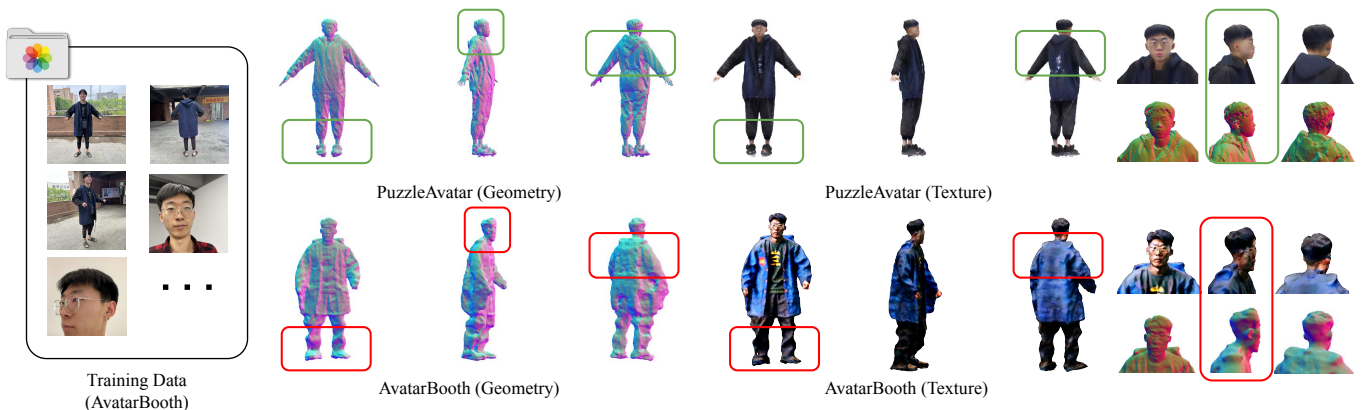
PuzzleAvatar ("asset 01> haircut")

PuzzleAvatar ("asset 02> face")

PuzzleAvatar w/ Detailed Description ("asset 01> short haircut")

PuzzleAvatar w/ Detailed Description ("asset 02> oval face")

Fig. 9. **Detailed vs. Plain Prompt Token** <asset X> suffices to maintain the appearance of assets. Elaborate prompts could introduce bias and hallucination.



PuzzleAvatar (Geometry)

PuzzleAvatar (Texture)

Training Data (AvatarBooth)

AvatarBooth (Geometry)

AvatarBooth (Texture)

Fig. 10. **AvatarBooth [Zeng et al. 2023] vs. PuzzleAvatar** AvatarBooth introduces a similar task, but overlooks the compositionality of garments and utilizes two separate DreamBooths (Head, Body) along with ControlNet, making it more complex and less scalable than PuzzleAvatar.

REFERENCES

- Thiemo Alldieck, Marcus A. Magnor, Weipeng Xu, Christian Theobalt, and Gerard Pons-Moll. 2018a. Detailed Human Avatars from Monocular Video. In *International Conference on 3D Vision (3DV)*.
- Thiemo Alldieck, Marcus A. Magnor, Weipeng Xu, Christian Theobalt, and Gerard Pons-Moll. 2018b. Video Based Reconstruction of 3D People Models. In *Computer Vision and Pattern Recognition (CVPR)*.
- Nikos Athanasiou, Mathis Petrovich, Michael J. Black, and Gül Varol. 2023. SINC: Spatial Composition of 3D Human Motions for Simultaneous Action Generation. *International Conference on Computer Vision (ICCV)* (2023).
- Omri Avrahami, Kfir Aberman, Ohad Fried, Daniel Cohen-Or, and Dani Lischinski. 2023. Break-A-Scene: Extracting Multiple Concepts from a Single Image. In *SIGGRAPH Asia 2023 Conference Papers (SA '23)*.
- Gwangbin Bae and Andrew J. Davison. 2024. Rethinking Inductive Biases for Surface Normal Estimation. In *Computer Vision and Pattern Recognition (CVPR)*.
- Wenjing Bian, Zirui Wang, Kejie Li, Jia-Wang Bian, and Victor Adrian Prisacariu. 2023. Nope-nerf: Optimising neural radiance field with no pose prior. In *Computer Vision and Pattern Recognition (CVPR)*.
- Tim Brooks, Bill Peebles, Connor Holmes, Will DePue, Yufei Guo, Li Jing, David Schnurr, Joe Taylor, Troy Luhman, Eric Luhman, Clarence Ng, Ricky Wang, and Aditya Ramesh. 2024. Video generation models as world simulators. (2024).
- Zhongang Cai, Daxuan Ren, Ailing Zeng, Zhengyu Lin, Tao Yu, Wenjia Wang, Xiangyu Fan, Yang Gao, Yifan Yu, Liang Pan, Fangzhou Hong, Mingyuan Zhang, Chen Change Loy, Lei Yang, and Ziwei Liu. 2022. HuMMan: Multi-modal 4D human dataset for versatile sensing and modeling. In *European Conference on Computer Vision (ECCV)*.
- Yukang Cao, Yan-Pei Cao, Kai Han, Ying Shan, and Kwan-Yee K Wong. 2024. DreamAvatar: Text-and-Shape Guided 3D Human Avatar Generation via Diffusion Models. *Computer Vision and Pattern Recognition (CVPR)* (2024).
- Pradyumna Chari, Sizhuo Ma, Daniil Ostashev, Achuta Kadambi, Gurunandan Krishnan, Jian Wang, and Kfir Aberman. 2023. Personalized Restoration via Dual-Pivot Tuning. *arXiv preprint arXiv:2312.17234* (2023).
- Mingjin Chen, Junhao Chen, Xiaojun Ye, Huan-ang Gao, Xiaoxue Chen, Zhaoxin Fan, and Hao Zhao. 2024. Ultraman: Single Image 3D Human Reconstruction with Ultra Speed and Detail. *arXiv preprint arXiv:2403.12028* (2024).
- Rui Chen, Yongwei Chen, Ningxin Jiao, and Kui Jia. 2023. Fantasia3D: Disentangling Geometry and Appearance for High-quality Text-to-3D Content Creation. In *International Conference on Computer Vision (ICCV)*.
- Wei Cheng, Ruixiang Chen, Wanqi Yin, Siming Fan, Keyu Chen, Honglin He, Huiwen Luo, Zhongang Cai, Jingbo Wang, Yang Gao, Zhengming Yu, Zhengyu Lin, Daxuan Ren, Lei Yang, Ziwei Liu, Chen Change Loy, Chen Qian, Wayne Wu, Dahua Lin, Bo Dai, and Kwan-Yee Lin. 2023. DNA-Rendering: A Diverse Neural Actor Repository for High-Fidelity Human-centric Rendering. In *International Conference on Computer Vision (ICCV)*.
- Matt Deitke, Dustin Schwenk, Jordi Salvador, Luca Weihs, Oscar Michel, Eli VanderBilt, Ludwig Schmidt, Kianna Ehsani, Anirudha Kembhavi, and Ali Farhadi. 2023. Objaverse: A universe of annotated 3d objects. In *Computer Vision and Pattern Recognition (CVPR)*.
- Yao Feng, Vasileios Choutas, Timo Bolkart, Dimitrios Tzionas, and Michael J. Black. 2021. Collaborative Regression of Expressive Bodies using Moderation. In *International Conference on 3D Vision (3DV)*.
- Yao Feng, Jinlong Yang, Marc Pollefeys, Michael J. Black, and Timo Bolkart. 2022. Capturing and Animation of Body and Clothing from Monocular Video. In *SIGGRAPH Asia 2022 Conference Papers (SA '22)*.
- Xiao Fu, Wei Yin, Mu Hu, Kaixuan Wang, Yuexin Ma, Ping Tan, Shaojie Shen, Dahua Lin, and Xiaoxiao Long. 2024b. GeoWizard: Unleashing the Diffusion Priors for 3D Geometry Estimation from a Single Image. *arXiv preprint arXiv:2403.12013* (2024).
- Yang Fu, Sifei Liu, Amey Kulkarni, Jan Kautz, Alexei A Efros, and Xiaolong Wang. 2024a. COLMAP-Free 3D Gaussian Splatting. *Computer Vision and Pattern Recognition (CVPR)* (2024).
- Gege Gao, Weiyang Liu, Anpei Chen, Andreas Geiger, and Bernhard Schölkopf. 2024. GraphDreamer: Compositional 3D Scene Synthesis from Scene Graphs. In *Computer Vision and Pattern Recognition (CVPR)*.
- Jun Gao, Wenzheng Chen, Tommy Xiang, Alec Jacobson, Morgan McGuire, and Sanja Fidler. 2020. Learning deformable tetrahedral meshes for 3d reconstruction. *Conference on Neural Information Processing Systems (NeurIPS)* (2020).
- Xiangjun Gao, Xiaoyu Li, Chaopeng Zhang, Qi Zhang, Yanpei Cao, Ying Shan, and Long Quan. 2023. ConTex-Human: Free-View Rendering of Human from a Single Image with Texture-Consistent Synthesis. *arXiv preprint arXiv:2311.17123* (2023).
- Marc Habermann, Weipeng Xu, Michael Zollhoefer, Gerard Pons-Moll, and Christian Theobalt. 2020. DeepCap: Monocular Human Performance Capture Using Weak Supervision. In *Computer Vision and Pattern Recognition (CVPR)*. IEEE.
- Fangzhou Hong, Mingyuan Zhang, Liang Pan, Zhongang Cai, Lei Yang, and Ziwei Liu. 2022. Avatarclip: Zero-shot text-driven generation and animation of 3d avatars. *Transactions on Graphics (TOG)* (2022).
- Xin Huang, Ruizhi Shao, Qi Zhang, Hongwen Zhang, Ying Feng, Yebin Liu, and Qing Wang. 2024a. HumanNorm: Learning normal diffusion model for high-quality and realistic 3d human generation. *Computer Vision and Pattern Recognition (CVPR)* (2024).
- Yukun Huang, Jianan Wang, Ailing Zeng, He Cao, Xianbiao Qi, Yukai Shi, Zheng-Jun Zha, and Lei Zhang. 2023a. DreamWaltz: Make a Scene with Complex 3D Animatable Avatars. In *Conference on Neural Information Processing Systems (NeurIPS)*.
- Yangyi Huang, Hongwei Yi, Weiyang Liu, Haofan Wang, Boxi Wu, Wenxiao Wang, Binbin Lin, Debing Zhang, and Deng Cai. 2023b. One-shot Implicit Animatable Avatars with Model-based Priors. In *International Conference on Computer Vision (ICCV)*.
- Yangyi Huang, Hongwei Yi, Yuliang Xiu, Tingting Liao, Jiayang Tang, Deng Cai, and Justus Thies. 2024b. TeCH: Text-guided Reconstruction of Lifelike Clothed Humans. In *International Conference on 3D Vision (3DV)*.
- Zeng Huang, Yuanlu Xu, Christoph Lassner, Hao Li, and Tony Tung. 2020. ARCH: Animatable Reconstruction of Clothed Humans. In *Computer Vision and Pattern Recognition (CVPR)*.
- Mustafa İşık, Martin Rünz, Markos Georgopoulos, Taras Khakhulin, Jonathan Starck, Lourdes Agapito, and Matthias Nießner. 2023. HumanRF: High-Fidelity Neural Radiance Fields for Humans in Motion. *Transactions on Graphics (TOG)* (2023).
- Ajay Jain, Ben Mildenhall, Jonathan T. Barron, Pieter Abbeel, and Ben Poole. 2022. Zero-Shot Text-Guided Object Generation with Dream Fields. In *Computer Vision and Pattern Recognition (CVPR)*.
- Oren Katzir, Or Patashnik, Daniel Cohen-Or, and Dani Lischinski. 2024. Noise-free Score Distillation. In *International Conference on Learning Representations (ICLR)*.
- Bingxin Ke, Anton Obukhov, Shengyu Huang, Nando Metzger, Rodrigo Caye Daudt, and Konrad Schindler. 2024. Repurposing diffusion-based image generators for monocular depth estimation. *Computer Vision and Pattern Recognition (CVPR)* (2024).
- Alexander Kirillov, Eric Mintun, Nikhila Ravi, Hanzi Mao, Chloe Rolland, Laura Gustafson, Tete Xiao, Spencer Whitehead, Alexander C Berg, Wan-Yen Lo, et al. 2023. Segment anything. In *International Conference on Computer Vision (ICCV)*.
- Peter Kocsis, Vincent Sitzmann, and Matthias Nießner. 2024. Intrinsic Image Diffusion for Single-view Material Estimation. In *Computer Vision and Pattern Recognition (CVPR)*.
- Nikos Kolotouros, Thiemo Alldieck, Andrei Zanfir, Eduard Gabriel Bazavan, Mihai Fieraru, and Cristian Sminchisescu. 2023. DreamHuman: Animatable 3D Avatars from Text. In *Conference on Neural Information Processing Systems (NeurIPS)*.
- Nupur Kumari, Bingliang Zhang, Richard Zhang, Eli Shechtman, and Jun-Yan Zhu. 2023. Multi-Concept Customization of Text-to-Image Diffusion. *Computer Vision and Pattern Recognition (CVPR)* (2023).
- Junnan Li, Dongxu Li, Caiming Xiong, and Steven Hoi. 2022. Blip: Bootstrapping language-image pre-training for unified vision-language understanding and generation. In *International Conference on Machine Learning (ICML)*. PMLR.
- Ruilong Li, Yuliang Xiu, Shunsuke Saito, Zeng Huang, Kyle Olszewski, and Hao Li. 2020. Monocular real-time volumetric performance capture. In *European Conference on Computer Vision (ECCV)*.
- Ruilong Li, Shan Yang, David A Ross, and Angjoo Kanazawa. 2021. Ai choreographer: Music conditioned 3d dance generation with aist++. In *International Conference on Computer Vision (ICCV)*.
- Zhen Li, Mingdeng Cao, Xintao Wang, Zhongang Qi, Ming-Ming Cheng, and Ying Shan. 2024. PhotoMaker: Customizing Realistic Human Photos via Stacked ID Embedding. In *Computer Vision and Pattern Recognition (CVPR)*.
- Jiang Liangze and Tao Lin. 2023. Test-Time Robust Personalization for Federated Learning. In *International Conference on Learning Representations (ICLR)*.
- Tingting Liao, Hongwei Yi, Yuliang Xiu, Jiayang Tang, Yangyi Huang, Justus Thies, and Michael J. Black. 2024. TADA! Text to Animatable Digital Avatars. In *International Conference on 3D Vision (3DV)*.
- Chen-Hsuan Lin, Wei-Chiu Ma, Antonio Torralba, and Simon Lucey. 2021. Barf: Bundle-adjusting neural radiance fields. In *International Conference on Computer Vision (ICCV)*.
- Lixiang Lin, Songyou Peng, Qijun Gan, and Jianke Zhu. 2024. FastHuman: Reconstructing High-Quality Clothed Human in Minutes. In *International Conference on 3D Vision, 3DV*.
- Ruoshi Liu, Rundi Wu, Basile Van Hoorick, Pavel Tokmakov, Sergey Zakharov, and Carl Vondrick. 2023. Zero-1-to-3: Zero-shot One Image to 3D Object. In *International Conference on Computer Vision (ICCV)*.
- Weiyang Liu, Zeru Qiu, Yao Feng, Yuliang Xiu, Yuxuan Xue, Longhui Yu, Haiwen Feng, Zhen Liu, Juyeeon Heo, Songyou Peng, Yangdong Wen, Michael J. Black, Adrian Weller, and Bernhard Schölkopf. 2024b. Parameter-Efficient Orthogonal Finetuning via Butterfly Factorization. *International Conference on Learning Representations (ICLR)* (2024).
- Zhen Liu, Yao Feng, Yuliang Xiu, Weiyang Liu, Liam Paull, Michael J. Black, and Bernhard Schölkopf. 2024a. Ghost on The Shell: An Expressive Representation of General 3D Shapes. *International Conference on Learning Representations (ICLR)* (2024).
- Simian Luo, Yiqin Tan, Longbo Huang, Jian Li, and Hang Zhao. 2023. Latent Consistency Models: Synthesizing High-Resolution Images with Few-Step Inference.

- arXiv:2310.04378
- Qianli Ma, Jinlong Yang, Anurag Ranjan, Sergi Pujades, Gerard Pons-Moll, Siyu Tang, and Michael J. Black. 2020. Learning to Dress 3D People in Generative Clothing. In *Computer Vision and Pattern Recognition (CVPR)*.
- Naureen Mahmood, Nima Ghorbani, Nikolaus F. Troje, Gerard Pons-Moll, and Michael J. Black. 2019. AMASS: Archive of Motion Capture as Surface Shapes. In *International Conference on Computer Vision (ICCV)*.
- Ricardo Martin-Brualla, Noha Radwan, Mehdi SM Sajjadi, Jonathan T Barron, Alexey Dosovitskiy, and Daniel Duckworth. 2021. Nerf in the wild: Neural radiance fields for unconstrained photo collections. In *Computer Vision and Pattern Recognition (CVPR)*.
- Andreas Meuleman, Yu-Lun Liu, Chen Gao, Jia-Bin Huang, Changil Kim, Min H Kim, and Johannes Kopf. 2023. Progressively optimized local radiance fields for robust view synthesis. In *Computer Vision and Pattern Recognition (CVPR)*.
- Ben Mildenhall, Pratul P Srinivasan, Matthew Tancik, Jonathan T Barron, Ravi Ramamoorthi, and Ren Ng. 2021. Nerf: Representing scenes as neural radiance fields for view synthesis. *Commun. ACM* (2021).
- OpenAI. 2023. GPT-4V(ision) system card.
- Priyanka Patel, Chun-Hao Paul Huang, Joachim Tesch, David Hoffmann, Shashank Tripathi, and Michael J. Black. 2021. AGORA: Avatars in Geography Optimized for Regression Analysis. In *Computer Vision and Pattern Recognition (CVPR)*.
- Georgios Pavlakos, Vasileios Choutas, Nima Ghorbani, Timo Bolkart, Ahmed AA Osman, Dimitrios Tzionas, and Michael J Black. 2019. Expressive body capture: 3d hands, face, and body from a single image. In *Computer Vision and Pattern Recognition (CVPR)*.
- Sida Peng, Chen Geng, Yuanqing Zhang, Yinghao Xu, Qianqian Wang, Qing Shuai, Xiaowei Zhou, and Hujun Bao. 2023. Implicit Neural Representations with Structured Latent Codes for Human Body Modeling. *Transactions on Pattern Analysis and Machine Intelligence (TPAMI)* (2023).
- Ben Poole, Ajay Jain, Jonathan T Barron, and Ben Mildenhall. 2023. DreamFusion: Text-to-3d using 2d diffusion. In *International Conference on Learning Representations (ICLR)*.
- Alec Radford, Jong Wook Kim, Chris Hallacy, Aditya Ramesh, Gabriel Goh, Sandhini Agarwal, Girish Sastry, Amanda Askell, Pamela Mishkin, Jack Clark, Gretchen Krueger, and Ilya Sutskever. 2021. Learning Transferable Visual Models From Natural Language Supervision. In *International Conference on Machine Learning (ICML)*. PMLR.
- Tianhe Ren, Shilong Liu, Ailing Zeng, Jing Lin, Kunchang Li, He Cao, Jiayu Chen, Xinyu Huang, Yukang Chen, Feng Yan, Zhaoyang Zeng, Hao Zhang, Feng Li, Jie Yang, Hongyang Li, Qing Jiang, and Lei Zhang. 2024. Grounded SAM: Assembling Open-World Models for Diverse Visual Tasks. arXiv:2401.14159 [cs.CV]
- Robin Rombach, Andreas Blattmann, Dominik Lorenz, Patrick Esser, and Björn Ommer. 2022. High-resolution image synthesis with latent diffusion models. In *Computer Vision and Pattern Recognition (CVPR)*.
- Nataniel Ruiz, Yuanzhen Li, Varun Jampani, Yael Pritch, Michael Rubinstein, and Kfir Aberman. 2023. DreamBooth: Fine tuning text-to-image diffusion models for subject-driven generation. In *Computer Vision and Pattern Recognition (CVPR)*.
- Shunsuke Saito, Zeng Huang, Ryota Natsume, Shigeo Morishima, Hao Li, and Angjoo Kanazawa. 2019. PIFu: Pixel-Aligned Implicit Function for High-Resolution Clothed Human Digitization. In *International Conference on Computer Vision (ICCV)*.
- Shunsuke Saito, Tomas Simon, Jason Saragih, and Hanbyul Joo. 2020. PIFuHD: Multi-Level Pixel-Aligned Implicit Function for High-Resolution 3D Human Digitization. In *Computer Vision and Pattern Recognition (CVPR)*.
- Kaiyue Shen, Chen Guo, Manuel Kaufmann, Juan Zarate, Julien Valentin, Jie Song, and Otmar Hilliges. 2023. X-Avatar: Expressive Human Avatars. In *Computer Vision and Pattern Recognition (CVPR)*.
- Tianchang Shen, Jun Gao, Kangxue Yin, Ming-Yu Liu, and Sanja Fidler. 2021. Deep marching tetrahedra: a hybrid representation for high-resolution 3d shape synthesis. *Conference on Neural Information Processing Systems (NeurIPS)* (2021).
- Yichun Shi, Peng Wang, Jianglong Ye, Long Mai, Kejie Li, and Xiao Yang. 2024. MV-Dream: Multi-view Diffusion for 3D Generation. *International Conference on Learning Representations (ICLR)* (2024).
- Sanghyun Son, Mathieu Gadelha, Yang Zhou, Zexiang Xu, Ming C. Lin, and Yi Zhou. 2024. DMesh: A Differentiable Representation for General Meshes. arXiv:2404.13445 [cs.CV]
- Yang Song, Prafulla Dhariwal, Mark Chen, and Ilya Sutskever. 2023. Consistency models. In *International Conference on Machine Learning (ICML)*.
- Jiaming Sun, Xi Chen, Qianqian Wang, Zhengqi Li, Hadar Averbuch-Elor, Xiaowei Zhou, and Noah Snavely. 2022. Neural 3D Reconstruction in the Wild. In *SIGGRAPH Conference Proceedings*.
- Jiaxiang Tang, Zhaoxi Chen, Xiaokang Chen, Tengfei Wang, Gang Zeng, and Ziwei Liu. 2024. LGM: Large Multi-View Gaussian Model for High-Resolution 3D Content Creation. arXiv preprint arXiv:2402.05054 (2024).
- Yoad Tewel, Omri Kaduri, Rinon Gal, Yoni Kasten, Lior Wolf, Gal Chechik, and Yuval Atzmon. 2024. ConsiStory: Training-Free Consistent Text-to-Image Generation. In *International Conference on Computer Graphics and Interactive Techniques (SIGGRAPH)*.
- Daniel Vlasic, Pieter Peers, Ilya Baran, Paul Debevec, Jovan Popović, Szymon Rusinkiewicz, and Wojciech Matusik. 2009. Dynamic shape capture using multi-view photometric stereo. In *ACM SIGGRAPH Asia 2009 Papers*.
- Haochen Wang, Xiaodan Du, Jiahao Li, Raymond A Yeh, and Greg Shakhnarovich. 2023a. Score Jacobian Chaining: Lifting Pretrained 2D Diffusion Models for 3D Generation. In *Computer Vision and Pattern Recognition (CVPR)*.
- Jionghao Wang, Yuan Liu, Zhiyang Dou, Zhengming Yu, Yongqing Liang, Xin Li, Wenping Wang, Rong Xie, and Li Song. 2023b. Disentangled Clothed Avatar Generation from Text Descriptions. arXiv preprint arXiv:2312.05295 (2023).
- Peng Wang, Hao Tan, Sai Bi, Yinghao Xu, Fujun Luan, Kalyan Sunkavalli, Wenping Wang, Zexiang Xu, and Kai Zhang. 2024c. PF-LRM: Pose-Free Large Reconstruction Model for Joint Pose and Shape Prediction. In *International Conference on Learning Representations (ICLR)*.
- Qixun Wang, Xu Bai, Haofan Wang, Zekui Qin, and Anthony Chen. 2024a. InstantID: Zero-shot Identity-Preserving Generation in Seconds. arXiv preprint arXiv:2401.07519 (2024).
- Shuzhe Wang, Vincent Leroy, Yohann Cabon, Boris Chidlovskii, and Revaud Jerome. 2024b. DUST3R: Geometric 3D Vision Made Easy. *Computer Vision and Pattern Recognition (CVPR)* (2024).
- Xintao Wang, Liangbin Xie, Ke Yu, Kelvin C.K. Chan, Chen Change Loy, and Chao Dong. 2022. BasicSR: Open Source Image and Video Restoration Toolbox.
- Zirui Wang, Shangzhe Wu, Weidi Xie, Min Chen, and Victor Adrian Prisacariu. 2021. NeRF-: Neural radiance fields without known camera parameters. arXiv preprint arXiv:2102.07064 (2021).
- Chung-Yi Weng, Brian Curless, Pratul P. Srinivasan, Jonathan T. Barron, and Ira Kemelmacher-Shlizerman. 2022. HumanNeRF: Free-Viewpoint Rendering of Moving People From Monocular Video. In *Computer Vision and Pattern Recognition (CVPR)*.
- Rundi Wu, Ben Mildenhall, Philipp Henzler, Keunhong Park, Ruiqi Gao, Daniel Watson, Pratul P. Srinivasan, Dor Verbin, Jonathan T. Barron, Ben Poole, and Aleksander Holynski. 2024. ReconFusion: 3D Reconstruction with Diffusion Priors. *Computer Vision and Pattern Recognition (CVPR)*.
- Yitong Xia, Hao Tang, Radu Timofte, and Luc Van Gool. 2022. Sinerf: Sinusoidal neural radiance fields for joint pose estimation and scene reconstruction. In *British Machine Vision Conference (BMVC)*.
- Enze Xie, Wenhai Wang, Zhiding Yu, Anima Anandkumar, Jose M Alvarez, and Ping Luo. 2021. SegFormer: Simple and efficient design for semantic segmentation with transformers. In *Conference on Neural Information Processing Systems (NeurIPS)*.
- Zhangyang Xiong, Chenghong Li, Kenkun Liu, Hongjie Liao, Jianqiao Hu, Junyi Zhu, Shuliang Ning, Lingteng Qiu, Chongjie Wang, Shijie Wang, et al. 2024. MVHumanNet: A Large-scale Dataset of Multi-view Daily Dressing Human Captures. In *Computer Vision and Pattern Recognition (CVPR)*.
- Yuliang Xiu, Jinlong Yang, Xu Cao, Dimitrios Tzionas, and Michael J. Black. 2023. ECON: Explicit Clothed humans Optimized via Normal integration. In *Computer Vision and Pattern Recognition (CVPR)*.
- Yuliang Xiu, Jinlong Yang, Dimitrios Tzionas, and Michael J. Black. 2022. ICON: Implicit Clothed humans Obtained from Normals. In *Computer Vision and Pattern Recognition (CVPR)*.
- Xihe Yang, Xingyu Chen, Daiheng Gao, Shaohui Wang, Xiaoguang Han, and Baoyuan Wang. 2024. HAVE-FUN: Human Avatar Reconstruction from Few-Shot Unconstrained Images. In *Computer Vision and Pattern Recognition (CVPR)*.
- Xueting Yang, Yihao Luo, Yuliang Xiu, Wei Wang, Hao Xu, and Zhaoxin Fan. 2023. D-IF: Uncertainty-aware Human Digitization via Implicit Distribution Field. In *International Conference on Computer Vision (ICCV)*.
- Tao Yu, Zerong Zheng, Kaiwen Guo, Pengpeng Liu, Qionghai Dai, and Yebin Liu. 2021. In *Computer Vision and Pattern Recognition (CVPR)*.
- Ye Yuan, Xueting Li, Yangyi Huang, Shalini De Mello, Koki Nagano, Jan Kautz, and Umar Iqbal. 2023. GAvatar: Animatable 3D Gaussian Avatars with Implicit Mesh Learning. arXiv preprint arXiv:2312.11461 (2023).
- Yifei Zeng, Yuanxun Lu, Xinya Ji, Yao Yao, Hao Zhu, and Xun Cao. 2023. AvatarBooth: High-Quality and Customizable 3D Human Avatar Generation. arXiv:2306.09864 (2023).
- Chao Zhang, Sergi Pujades, Michael Black, and Gerard Pons-Moll. 2017. Detailed, accurate, human shape estimation from clothed 3D scan sequences. In *Computer Vision and Pattern Recognition (CVPR)*.
- Jingbo Zhang, Xiaoyu Li, Qi Zhang, Yanpei Cao, Ying Shan, and Jing Liao. 2023. HumanRef: Single Image to 3D Human Generation via Reference-Guided Diffusion. arXiv preprint arXiv:2311.16961 (2023).
- Jason Y Zhang, Amy Lin, Moneish Kumar, Tzu-Hsuan Yang, Deva Ramanan, and Shubham Tulsiani. 2024. Cameras as Rays: Pose Estimation via Ray Diffusion. In *International Conference on Learning Representations (ICLR)*.
- Lvmin Zhang and Maneesh Agrawala. 2023. Adding Conditional Control to Text-to-Image Diffusion Models. In *International Conference on Computer Vision (ICCV)*.

- Zerong Zheng, Tao Yu, Yebin Liu, and Qionghai Dai. 2021. PaMIR: Parametric Model-conditioned Implicit Representation for image-based human reconstruction. *Transactions on Pattern Analysis and Machine Intelligence (TPAMI)* (2021).
- Zerong Zheng, Tao Yu, Yixuan Wei, Qionghai Dai, and Yebin Liu. 2019. DeepHuman: 3D Human Reconstruction From a Single Image. In *International Conference on Computer Vision (ICCV)*.

A GPT-4V PROMPT FOR PUZZLEBOOTH

Queried Prompt. *“Analyze the provided images, each featuring an individual. Identify and describe the individual’s gender, facial features (excluding hair), haircut, and specific clothing items such as shirts, hats, pants, shoes, dresses, skirts, scarves, etc. Return the results in a dictionary format with keys for "gender", "face", "haircut", and each type of clothing. The corresponding value should provide 1-3 adjective or noun words, which describe the topological or geometric features, such as length (e.g., short, long, midi, mini, knee-length, floor length, ankle-length, hip-length, calf-length), shape (e.g., oval, round, square, heart-shaped, diamond-shaped, rectangular, voluminous, razor-cut, tousled, layered, messy), tightness (e.g., tight, snug, fitted, skin-tight, loose, tight-fitting, clingy), style (e.g., modern, casual, sporty, classic, formal, vintage, bohemian, avant-garde), or haircut types (e.g., long, short, wavy, straight, curly, bald, medium-length, pony tail, bun, plaits, beard, sideburns, dreadlocks, goatee), without referencing color or texture pattern. Exclude accessories and don’t include any clothing item in the description of another. Omit any keys for which the clothing item does not appear or the description is empty. The response should be a dictionary only, without any additional sentences, explanations, or markdowns syntax (like json)”*

B CAMERA SETTING

To familiarize the diffusion model with the camera positions sampled during SDS optimization, we rendered the synthetic color-normal image pairs in the exact same manner as the SDS sampling strategy. This rendered data will be used in preserving synthetic human prior ($\mathcal{L}_{\text{prior}}$), while training the 2D generator G_{puzzle} .

To ensure complete coverage of the entire body and face, we sample virtual camera poses around the full body and zoom in on the face region. To reduce the occurrence of mirrored appearance artifacts (e.g., Janus-head), we incorporated view-aware prompts (i.e., “front/side/back/overhead view”), regarding the viewing angle during the generation process. The effectiveness of this approach has been demonstrated in DreamFusion [Poole et al. 2023].

To ensure full coverage of the entire body and the human face, we sample virtual camera poses into two groups: 1) \mathbf{K}_{body} cameras with a field of view (FOV) covering the full body or the main body parts, and 2) zoom-in cameras \mathbf{K}_{face} focusing the face region.

The ratio $\mathcal{P}_{\text{body}}$ determines the probability of sampling $\mathbf{k} \in \mathbf{K}_{\text{body}}$, while the height h_{body} , radius r_{body} , elevation angle ϕ_{body} , and azimuth ranges θ_{body} are adjusted relative to the SMPL-X body scale. Empirically, we set $\mathcal{P}_{\text{body}} = 0.5$, $h_{\text{body}} = [-0.4, 0.4]$, $r_{\text{body}} = (0.7, 1.3)$, $\theta_{\text{body}} = [60^\circ, 120^\circ]$, $\phi_{\text{body}} = [0^\circ, 360^\circ]$, with the M_{body} proportionally scaled to a $[-0.5, 0.5]$ unit space.

To enhance facial details, we sample additional virtual cameras positioned around the face $\mathbf{k} \in \mathbf{K}_{\text{face}}$, together with the additional prompt “face of”. With a probability of $\mathcal{P}_{\text{face}} = 1 - \mathcal{P}_{\text{body}} = 0.5$, the sampling parameters include the view target c_{face} , radius range r_{face} , rotation range θ_{face} , and azimuth range ϕ_{face} . Empirically, we set c_{face} to the 3D position of SMPL-X head keypoint, $r_{\text{face}} = [0.3, 0.4]$, $\theta_{\text{face}} = [90^\circ, 90^\circ]$ and $\phi_{\text{face}} = [-90^\circ, 90^\circ]$.

Regarding the synthetic data, we use all the subjects (525 textured scans) in THuman2.0. For each subject, we render 8 full-body views and 8 head views, as shown in Fig. 4, and query their descriptive prompts via GPT-4V [OpenAI 2023]. This gives us $525 \times 8 \times 2 = 8400$ color-normal pairs in total.